Probabilistic Modeling of the Oxygen Saturation Pattern for the Detection of Anomalies During Clinical Interventions

D Martín Martínez, P Casaseca de la Higuera, M Martín Fernández, C Alberola López

Laboratory of Image Processing, Universidad de Valladolid, Valladolid, Spain

Abstract

In this paper, we propose a Markov model–based methodology aimed at detecting in real time the anomalies that the oxygen saturation pattern suffers during clinical interventions or procedures. To this end, we first extract a reference pattern from the patient in nominal conditions before the procedure takes place. Then, in a second stage, a measurement of the similarity between the reference pattern and the pattern of the epoch to be tested is obtained through the Williams' Index. This measurement is compared with a threshold to determine the normal/abnormal character of the pattern under test. Experiments on real data show that the proposed methodology is sensitive to the anomalies induced when the respiratory function is impaired; this is accomplished through the simulation of several situations (shortness of breath, interrupted breathing, hyperventilation and CO_2 increasing in blood) in which the respiratory impairment is manually emulated.

1. Introduction

Patient monitoring (ECG, blood pressure, pulse oximetry, etc.) constitutes a very useful tool for anomaly detection during large part of clinical interventions and procedures. However, its use is not extended in minor surgeries or some dental interventions due to the extremely low probability of complications, a fact that does not justify its high cost (either economic, temporal or both). Oxygen saturation (SaO_2) has been used as an inexpensive, noninvasive alternative since 1980's [1]. Despite its clear potential, it presents some limitations that prevent it from being massively used: SaO_2 readings are not easy to interpret and the measurements are usually distorted by a broad variety of factors such as ambient light and temperature [2]. Consequently, research efforts have focused on overcoming these limitations and to render the SaO_2 a valuable diagnostic procedure.

In this paper, we describe a novel analysis methodology, based on stochastic signal modeling, aimed to extract the SaO_2 pattern of any patient. In particular, this methodology detects the variations (consequence of clinical complications) that the aforementioned pattern suffers during a clinical intervention with respect to a reference pattern obtained from the patient before the intervention takes place. This approach circumvents the major part of the drawbacks associated to the use of SaO_2; specifically, (a) the interpretation of the reading is far simpler since we give a measure of deviation from the reference pattern; (b) the well–known biases [1–3] inherent to this sensing technique are avoided as a consequence of using the data so affected in the reference patterns; (c) the index on which our classifier is based does not require long signal records so it is amenable for realtime analysis, a feature that makes our proposal deviate from a substantial portion of the approaches reported in literature [4, 5].

The paper is structured as follows: Section 2 presents the proposed methodological approach, whereas Section 3 is devoted to illustrate the performance of the proposal by describing the set of experiments which have been carried out. Finally, section 4 closes the paper with a compilation of the findings drawn from this work.

2. Methods

2.1. Oxygen saturation signal modeling

Among the broad range of models that could be used for this sort of signals, we have selected Markov Models [6] for two main reasons:

1. The SaO_2 signal takes integer values between 0 and 100, which suggests an association between signal values and states of the model.
2. The variability of the signal (transitions between states) does not seem to be chaotic, but governed by a non-uniform probability law.

Since the states of the Markov model do not depend on the specific acquisitions, hereinafter, "the model" shall refer to the aforementioned probability law. Typically, this law is represented as a matrix whose (i, j) element denotes the transition probability from the $i-$th to the $j-$th state:

$$[p_{ij}]_{i,j} \in \mathcal{M}_{101\times101} \text{ with } \begin{matrix} i = 0, 1, \cdots, 100 \\ j = 0, 1, \cdots, 100. \end{matrix} \quad (1)$$

Considering that a 10–minute registry sampled at $f_s = 1$ Hz is composed of 600 samples, a model defined this way is highly impractical. The number of parameters of such a model would be $101 \times 101 = 10,201$, which would have to be estimated from the acquired data. In order to overcome this shortcoming, the following assumption can be made: only transitions between consecutive states can occur; those transitions between non–consecutive states are not considered real but artifacts derived from sampling continuous data. This assumption provides a substantial simplification to the model since the probability law can now be constructed from a lower number of transitions:

$$\overline{\overline{\mathcal{P}}} \equiv [p_{ij}]_{i,j} \in \mathcal{M}_{101\times 101}, \tag{2}$$

with non-null entries only in the main and both secondary diagonals ($i = 0, 1, \cdots, 100$ and $j = i-1, i, i+1$). This new matrix has only 301 parameters[1] to be estimated, which is affordable. Most $\mathrm{SaO_2}$ signals comply with this assumption. If this is not the case, a simple linear interpolation (and rounding) is enough to make any signal satisfy it:

$$x_{\mathrm{smooth}}[k] = \mathrm{round}\left(\mathrm{Interp}\left(x[\ell], M\right)\right), \tag{3}$$

where $k = M(\ell - 1) + 1$, and

$$M = \max\left\{\|\nabla^f \cdot x[\ell]\|,\ \forall \ell < L\right\} \tag{4}$$

is the interpolation rate[2].

As far as the parameter estimation is concerned, the occurrence probabilities of "non-explicit" transitions constitute an additional challenge — these transitions are those which do not appear on the registries—; four different scenarios can appear:

• **Scene 1:** *All the transitions are explicit.–* Their associated probabilities may be directly computed from the number of appearances on the registry.

• **Scene 2:** *Only two out of the three transitions are explicit.–* Bearing in mind that $\sum_j p_{ij} = 1$, a data-driven-only approach would make the probability of the non-explicit transition be zero, i.e., the unobserved transitions would not be considered possible[3], a result that would only be correct for infinitely long registries. To avoid this, we propose the following reassignment:

$$\begin{aligned} q_1/Q &\rightarrow q_1/(Q+1), \\ q_2/Q &\rightarrow q_2/(Q+1), \\ 0 &\rightarrow 1/(Q+1), \end{aligned}$$

where q_1 and q_2 ($q_1 + q_2 = Q$) are the number of explicit transitions. The rationale of that reassignment lies on the following concerns:

– The unobserved state should have a probability lower than $1/Q$; this explains the fact of being unobserved for such a registry.

– For larger values of Q (i.e., very accurate estimations), the new probabilities are close to the previous ones.

• **Scene 3:** *Only one among the three transitions is explicit.–* In this case, we propose a similar procedure to the previous one: $Q/Q \rightarrow Q/(Q+1)$ for the explicit transition, and

$$\alpha \cdot \exp\left(-d(S_D)\right) \tag{5}$$

for the non-explicit transitions, where $d(S_D)$ denotes the Euclidean distance between the destination state (S_D) and the closest explicit state, and α is the scale parameter aimed at ensuring the compliance with $\sum_j p_{ij} = 1$.

• **Scene 4:** *No transition is explicit.–* An exponential rule, similar to the one in (5) is proposed:

$$\alpha \cdot \exp\left(-\lambda \cdot d(S_D)\right), \tag{6}$$

where the parameter λ is set to $d(S_O)$, i.e., the Euclidean distance between the origin state and the closest explicit one. By defining this rule, we ensure that stochastic simulations of the model will rapidly evolve towards explicit states.

2.2. Classification methodology

As stated in section 1, the main objective of this work is to detect variations (with respect to a reference), of the $\mathrm{SaO_2}$ pattern during any clinical intervention in real time. To this end, we propose a classification methodology consisting of two stages, namely: 1) obtention of the reference and the testing pattern and 2) similarity assessment through the Williams' Index. A flow chart of the proposed methodology with explicit interconnection of these two stages is presented in Figure 1.

• **Obtaining the reference pattern.** The reference pattern can be defined as a set of models (see section 2.1) accounting for a patient acquisition under nominal conditions at a specific place and time. Each one of these models is obtained from a window of the registry which is defined as follows: given a $\mathrm{SaO_2}$ signal, denoted as $x[\ell]$[4] for $\ell = 1, 2, \cdots, L$ a set of N windows —$\{\mathbf{w}_{NC}[n]\}_{n=1}^{N}$— is created, where

$$\mathbf{w}_{NC}[n] = \begin{bmatrix} x[\tau(n-1)+1] \\ x[\tau(n-1)+2] \\ \vdots \\ x[\tau(n-1)+\mathcal{T}-1] \\ x[\tau(n-1)+\mathcal{T}] \end{bmatrix}^T, \quad \begin{array}{l} n \in \mathbb{N} \leq N \\ \mathcal{T} \in \mathbb{N} \geq 2 \\ \tau \in \mathbb{N} < \mathcal{T} \end{array}, \tag{7}$$

[1] The matrix is composed by 303 elements, but both $p_{0,-1}$ and $p_{100,101}$ are equal to zero as impossible transitions.

[2] ∇^f denotes de forward gradient

[3] This assertion finds its justification in the discrete nature of the sample space.

[4] $x[\ell] \in \mathbb{Z} \leq 100$, according to the $\mathrm{SaO_2}$ nature.

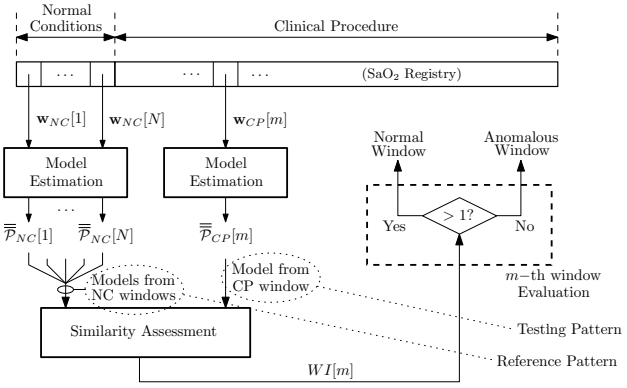

Figure 1. Flowchart of the proposed methodology for the detection of windows with anomalous $\mathrm{SaO_2}$ pattern. "NC" and "CP" denote "Normal Conditions" and "Clinical Procedure" respectively.

with τ and $\mathcal{T}$ the overlap parameter and the length of the window respectively[5]. Hence, the output of this stage is a set of N models:

$$\{\mathbf{w}_{NC}[n]\}_{n=1}^{N} \xrightarrow{\text{Modeling}} \left\{\overline{\overline{\mathcal{P}}}_{NC}[n]\right\}_{n=1}^{N}. \quad (8)$$

• **Obtaining the testing pattern.** The analysis of the registry acquired during the clinical procedure/intervention must be performed in the same manner as it was in the previous stage. That is, the registry is divided into windows which are subsequently used to estimate the corresponding models. This case, however, the testing pattern consists of just one model instead of a set of them. Hence, there is one testing pattern for each window: for the generic $m-$th window ($\mathbf{w}_{CP}[m]$), the model $\overline{\overline{\mathcal{P}}}_{CP}[m]$ is estimated.

• **Similarity assessment (Williams' Index).** The objective of this stage is to provide a measure of the similarity between the testing and the reference patterns. Our recent experience on signal modeling (PPG and ECG modeling [7, 8]) suggests the use of the Williams' Index [9] (hereafter WI) since the homogeneity/heterogeneity of the reference pattern is considered. This index determines how the testing pattern agrees with the reference patterns in comparison with how the models of the reference pattern agree with each other. Hence, WI ≥ 1 means that the testing pattern is, at least, as similar to the reference pattern as the models forming the reference pattern are with each other. So, WI ≥ 1 means the testing pattern is within the reference pattern, whilst WI < 1 means the testing pattern is far from the reference pattern. The WI is defined as

$$WI[m] = \frac{(N-1)\cdot \sum_{n=1}^{N} a\left(\overline{\overline{\mathcal{P}}}_{CP}[m], \overline{\overline{\mathcal{P}}}_{NC}[n]\right)}{2\cdot \sum_{n=1}^{N}\sum_{n'>n}^{N} a\left(\overline{\overline{\mathcal{P}}}_{NC}[n], \overline{\overline{\mathcal{P}}}_{NC}[n']\right)}, \quad (9)$$

where $a(\cdot\,,\cdot\,)$ is the agreement measurement. In this case, given that we are dealing with probability density functions, the agreement function is an approach based on the Kullback–Leibler divergence: the agreement for two models, $\overline{\overline{\mathcal{P}}}_1$ and $\overline{\overline{\mathcal{P}}}_2$, is defined as[6]

$$a\left(\overline{\overline{\mathcal{P}}}_1, \overline{\overline{\mathcal{P}}}_2\right) = \exp\left(-M_{KL}\left(\overline{\overline{\mathcal{P}}}_1, \overline{\overline{\mathcal{P}}}_2\right)\right), \quad (10)$$

where M_{KL} is a metric derived from the divergence as

$$M_{KL}\left(\overline{\overline{\mathcal{P}}}_1, \overline{\overline{\mathcal{P}}}_2\right) = D_{KL}\left(\overline{\overline{\mathcal{P}}}_1, \overline{\overline{\mathcal{P}}}_2\right) + D_{KL}\left(\overline{\overline{\mathcal{P}}}_2, \overline{\overline{\mathcal{P}}}_1\right),$$

and the divergence is computed as

$$D_{KL}\left(\overline{\overline{\mathcal{P}}}_1, \overline{\overline{\mathcal{P}}}_2\right) = \sum_{i=0}^{100}\sum_{j=i-1}^{i+1} (p_{i,j})_1 \ln\left(\frac{(p_{i,j})_1}{(p_{i,j})_2}\right). \quad (11)$$

3. Experiments and discussion

To illustrate the performance of our proposal, we present four experiments that emulate several situations in which the respiratory function is altered: shortness of breath, interrupted breath, hyperventilation and an increase of the $\mathrm{CO_2}$ level in blood. Each simulation is an operating procedure that involves alternating periods of normal conditions and periods during which the respiratory function is manually impaired.

The signals used in this section have been acquired with the Omicrom FT Surveyor (RGB Medical Devices LTD, see acknowledgement) with the sensor located in the patient's right index finger. All the acquisitions have been performing with a sampling frequency $f_s = 1$ Hz.

Results of all the experiments are presented in Figure 2, in which the original $\mathrm{SaO_2}$ signals are represented together with the associated Williams' Index series.

• **Exp. 1: Shortness of breath.** *Protocol: 5 minutes under normal conditions and 5 minutes with a tissue covering nose and mouth.* The Williams' Index drops off dramatically a minute after the beginning of the procedure (see Figure 2–(a)). This result could be expected, since the effects of covering nose and mouth with a tissue over the $\mathrm{SaO_2}$ are not immediate. It should be noted that the alteration suffered by the $\mathrm{SaO_2}$ pattern, which has been detected by our method, is not trivial to detect visually.

• **Exp. 2: Interrupted breathing.** *Protocol: 5 minutes under normal conditions and 3.5 minutes holding breath as much as possible.* This case, the alteration suffered by the pattern may be visually detected. However, these altered windows would not be labeled as "abnormal" without a deep characterization of the $\mathrm{SaO_2}$ pattern under normal conditions. Figure 2–(b) shows the sensitivity of the method, with Williams' Index values lower than one as soon as the effects of the interruption are noticeable on the $\mathrm{SaO_2}$ registry.

• **Exp. 3: Hyperventilation (HV).** *Protocol: 5 minutes under normal conditions, 1 minute breathing as fast as*

[5] Previous experiments suggest $\mathcal{T} = 20$ and $\tau = 5$ as appropriate values.

[6] $a(\cdot\,,\cdot\,) \in (0, 1]$ (see eq. (10)), which is a desirable feature according to the author of [9].

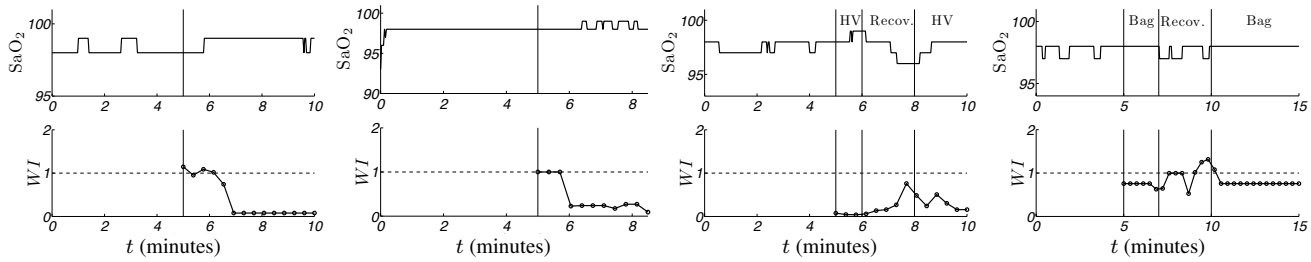

(a) Experiment 1 (b) Experiment 2 (c) Experiment 3 (d) Experiment 4

Figure 2. Experimental results. For each experiment, both the SaO_2 signals and the Williams' Index are represented.

possible, 2 minutes recovering (normal conditions) and another 2 minutes breathing as fast as possible. Despite the effect of this procedure can immediately be detected over the SaO_2 registry, once the normal ventilation is restored, the effects fade out slowly.

Figure 2–(c) shows how the effect of HV is detected immediately. However, once the HV ceases, the effects can still be noticed. This is reflected in the Williams' Index as an increasing tendency. After that, when the HV resumes, the Williams' Index falls down again.

- **Exp. 4: CO_2 increasing in blood.** *Protocol: 5 minutes under normal conditions, 2 minute breathing with a plastic bag covering nose and mouth, 3 minutes recovering (normal conditions) and additional 5 minutes breathing with a plastic bag.* This experiment has been included to illustrate the robustness against false positives, i.e., Williams' Index values lower than one for normal windows. To this end, we have evaluated a situation in which the patient recovers the normal pattern just a few seconds after the termination of the procedure. Results in Figure 2–(d) show that during the procedure, the Williams' Index is always below 1 and during the recovery interval, most of the index values (apart from some exceptions probably due to an incomplete recovery) are above that threshold.

4. Conclusions

We have introduced a novel analysis methodology, based on Markov Models, for detecting the alterations that the SaO_2 pattern suffers during a clinical intervention/procedure. Our methodology differs from most approaches reported so far in the following aspects: (a) readings are simpler as well as free from biases, and (b) it can be used in real time. In addition, we would like to highlight that the proposed model for the SaO_2 signal is also a contribution of the authors. Experimental results, show the sensitivity of our proposal to some situations in which the respiratory function is impaired. This fact is more relevant considering that, in some cases, the way that the impairment is reflected in the SaO_2 signal is not evident. Thus, we can conclude that the proposal here presented is a promising and inexpensive tool for patient monitoring during clinical interventions.

Acknowledgments

This work is partially supported by the Universidad de Valladolid and the Banco Santander under the FPI–UVa fellowship, the Spanish Ministerio de Ciencia e Innovación and the Fondo Europeo de Desarrollo Regional (FEDER) under Research Grant TEC2010-17982, the Spanish Instituto de Salud Carlos III (ISCIII) under Research Grants PI11-01492, PI11-02203 and by the Spanish Centro para el Desarrollo Tecnológico Industrial (CDTI) under the cvREMOD (CEN-20091044) project. Authors would like to thank the support of the company RGB Medical Devices LTD for kindly sharing us the measurement devices.

References

[1] Valdez-Lowe C, Ghareeb S, Artinian N. Pulse oximetry in adults. Am J Nurs 2009;109:52–59.

[2] Mendelson Y. Pulse oximetry: Theory and applications for noninvasive monitoring. Clin Chem 1992;38:1601–1607.

[3] Wukitsch M, Peterson M, Tobler D, Pologe J. Pulse oximetry: Analysis of theory, technology and practice. J Clin Monit 1988;4:290–301.

[4] Golemati S. Comparison of entropy measures for estimating severity of obstructive sleep apnea from overnight pulse oximetry data. In 10th IEEE Int Conf on Inf Tech and Appl in Biomed (ITAB), 2010. 2010; 1–4.

[5] Al-Angari H. Automated recognition of obstructive sleep apnea syndrome using support vector machine classifier. IEEE Trans Inf Theory 2012;16:463–468.

[6] Mohamed M, Gader P. Generalized hidden Markov models. I. Theoretical frameworks. IEEE Trans Fuzzy Sys 2000; 8:67–81.

[7] Martín-Martínez D, Casaseca-de-la-Higuera P, Martín-Fernández M, Alberola-López C. Cardiovascular signal reconstruction based on parameterization –shape modeling– and non-stationary temporal modeling. In Proc 20th Eur Sig Proc Conf. Bucharest, Romania, August 2012; 1826–1830.

[8] Martín-Martínez D, Casaseca-de-la-Higuera P, Martín-Fernández M, Alberola-López C. Stochastic modeling of the PPG signal: A synthesis–by–analysis approach with applications. IEEE Trans Biomed Eng 2013;In press.

[9] Williams G. Comparing the joint agreement of several raters with another rater. Biometrics 1976;32:619–627.